Available online at www.ijpcr.com
International Journal of Pharmaceutical and Clinical Research 2018; 10(1): 1-15

ISSN- 0975 1556

Research Article

Unraveling the Inhibitory Activities of *Gentiana* Derivatives Against Inflammatory Response of Rheumatoid Arthritis Using Molecular Modeling Approach

Matchado Monica Steffi[1], Sachidanand Singh[1,2], Arulmozhi S[1*]

[1]*Bioinformatics, Department of Biosciences and Technology, Karunya University, Coimbatore, Tamil Nadu*
[2]*Institute of Bioscience and Technology, Sri Ramswaroop University, Lucknow, Uttar Pradesh*

Received: 24th Mar, 17; Revised 13th Dec, 17, Accepted: 27th Dec, 17; Available Online:25th Jan, 18

ABSTRACT

Rheumatoid arthritis (RA) is a chronic autoimmune disorder which may cause joint deformity and bone erosion. Combined usage of anti-inflammatory and autoimmune drugs, leads to many side effects, due to which people suffering from RA are moving towards alternative treatment. Medicinal herbs can be a complementary and alternative medicine with less harmful effects. Qin-Jiao is the popular ancient Chinese herb usually used in the treatment of RA. Among the genus *Gentiana*, roots of *Gentiana macrophylla*, *Gentiana crassicaulis*, *Gentiana straminea*, and *Gentiana dahurica*, are characterized as Qin-Jiao. The aim of the present study is to understand the inhibitory effects of the compounds present in these *Gentiana* species. Twenty-one compounds from *G. dahurica* and twelve compounds from the other three *Gentiana species* were selected for molecular modeling studies using the Glide module of Maestro v 9.2. Out of the thirty-three compounds, seventeen compounds were docked against Cyclooxygenase-2 (COX-2) target protein. Among these compounds, $C_{27}H_{38}O_{19}$ showed the highest inhibitory effect with the docking score of -14.47 and glide energy of -68.43KcaL/mol. Stability of the docking complex COX-2 with the compound $C_{27}H_{38}O_{19}$ was also evaluated through Molecular Dynamics (MD) simulation studies using Desmond v4.0. Root mean square deviations and Root mean square fluctuations represented the stability of the docking complex. This approach underlines that this compound can be further evaluated at *in vivo* and *in vitro* studies as a mark of treatment for RA.

Keywords Rheumatoid Arthritis, *Gentiana dahurica*, Cyclooxygenase-2, Molecular docking, Molecular dynamics simulation.

INTRODUCTION

Rheumatoid Arthritis (RA) is a symmetric polyarticular arthritis which leads to inflammation in the synovium and destruction of local articular structures[1]. Among different types of autoimmune inflammatory arthritis, RA accounts for nearly 1% of the adult population worldwide. It mainly affects joints and with the disease progression, it also moves to the cardiovascular system, lungs and muscles[2-4]. The exact mechanism of the cause of the disease is still not fully revealed, but genetic susceptibility and environmental factors contribute an equal part in triggering the abnormal autoimmune response [5]. RA can be perpetuated by several factors which include proinflammatory cytokines, free radicals, interleukin (IL)-1β, T-cells, Tumor Necrosis Factor-α (TNF-α) and IL-6[6].

The disease progression of RA is associated with multiple target genes. Among these target genes, Cyclooxygenase (COX) plays a crucial role in the inflammatory process. COX-1 and COX-2 are two important isoenzymes of COX [7]. Proinflammatory cytokines, lipopolysaccharides and growth factors are responsible for stimulating the expression of COX. COX gene expression is directly correlated with inflammatory pathological processes, apoptosis, cancer and angiogenesis. Structural changes in COX lead to arthritic diseases[8-9]. High expression level of COX-2 was also reported in synovial tissues of rheumatoid arthritis patients[10]. COX has long hydrophobic residues in the active site region which can act as the binding pocket for anti-inflammatory drugs[11].

RA is being treated with several conventional drugs like nonsteroidal anti-inflammatory drugs (NSAID), glucocorticoids and disease-modifying anti-rheumatic drugs (DMARDs), which have the inhibitory effects on COX[12]. Long term usage of these drugs may result in several side effects like gastrointestinal disorders, weight loss, diarrhea, skin rashes, and alopecia[13]. Herbal medicinal treatment can be a potential alternative therapeutic approach towards RA with less side effects[14].

Qin-Jiao is known as the most popular potential and traditional Chinese medicinal herb which has been used mainly for the treatment of rheumatism. Qin-Jiao consists of four plant roots such as *Gentiana macrophylla*, *Gentiana crassicaulis*, *Gentiana straminea*, and *Gentiana dahurica*[15]. It also has significant effects on jaundice, diabetes mellitus, arthralgia, stroke, hemiplegia, paralysis, infantile malnutrition and pains[16]. Species of *Gentiana* are rich in iridoid glycosides, loganic acid, gentiopicroside, sweroside and swertiamarinin, among which

**Author for Correspondence: arulmozhisrinivasan74@gmail.com*

gentiopicroside is been reported as the inhibitor of nitric oxide (NO) and COX-2[17].

Gentiana dahurica is one of the most important constituents of Qin-Jiao and it is found in China and Mongolia. The roots of this plant are commonly used for

Table 1: Thirty-three compounds selected from Gentiana species.

S.no	Ligand structure	Molecular formula	Name
1	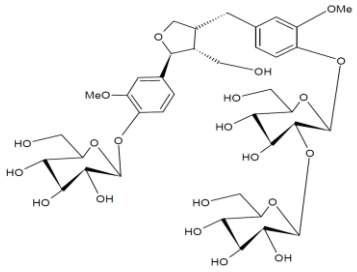	$C_{38}H_{54}O_{21}$	
2	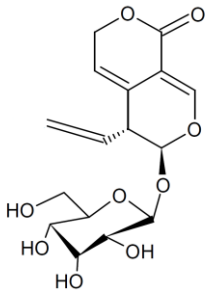	$C_{16}H_{20}O_9$	Gentiopicroside
3	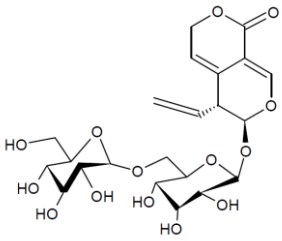	$C_{22}H_{30}O_{14}$	6′-O-β-D-glucopyranosyl gentiopicroside
4	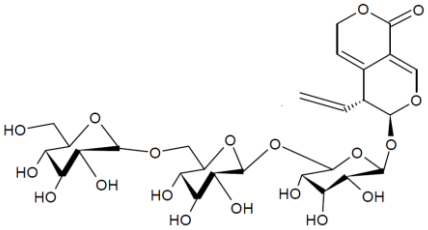	$C_{27}H_{38}O_{19}$	Scarban G3
5	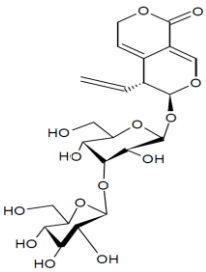	$C_{22}H_{30}O_{14}$	Olivieroside C
6	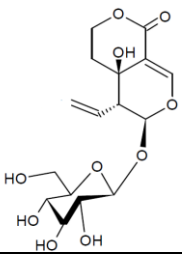	$C_{16}H_{22}O_{10}$	Swertiamarin

7	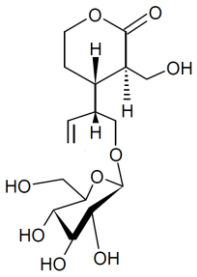	$C_{16}H_{26}O_9$	1-O-β-D-glucopyranosyl-amplexi
8	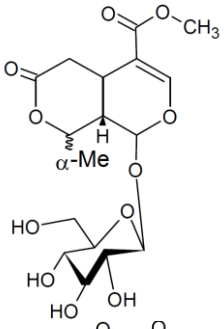	$C_{17}H_{24}O_{11}$	Epi-kingiside
9	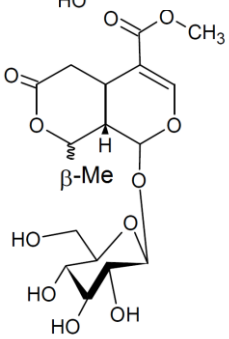	$C_{17}H_{24}O_{11}$	Kingiside
10	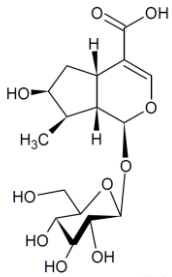	$C_{16}H_{24}O_{10}$	Loganic acid
11	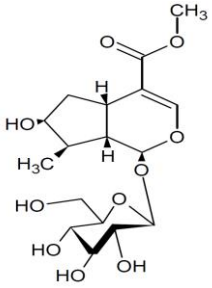	$C_{17}H_{26}O_{10}$	Loganin
12	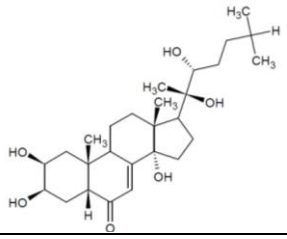	$C_{27}H_{44}O_6$	Ajugasterone C

13	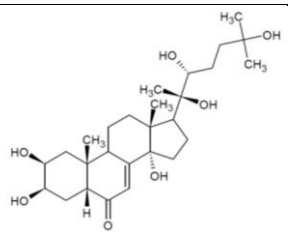	$C_{27}H_{44}O_7$	20-hydroxyecdysone
14	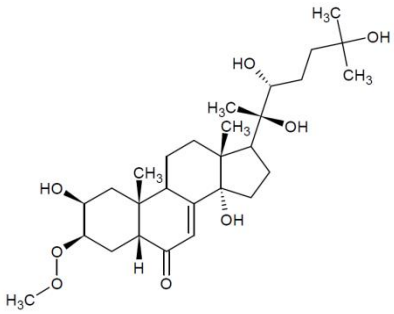	$C_{28}H_{46}O_8$	20-hydroxyecdysone 3-acetate
15	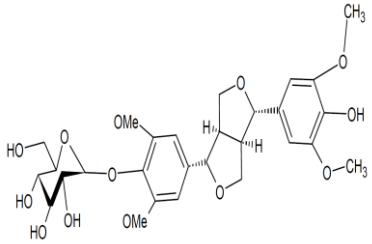	$C_{28}H_{36}O_{13}$	Syringaresinol-β-D-glucopyranoside
16	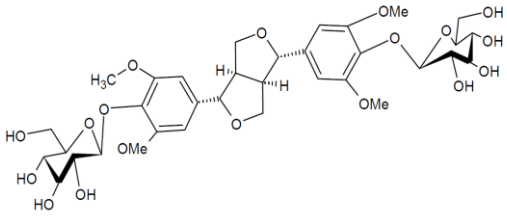	$C_{34}H_{46}O_{18}$	Liriodendrin
17	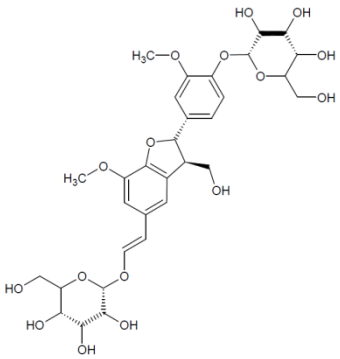	$C_{31}H_{40}O_{16}$	Dehydrodiconiferyl alcohol 4,γ′-di-O-β-D-glucopyranoside
18	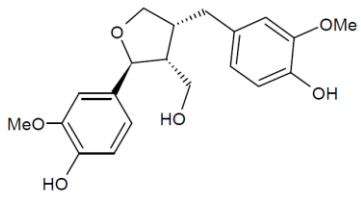	$C_{20}H_{24}O_6$	Lariciresinol-4′-O-β-D-glucopyranoside

19	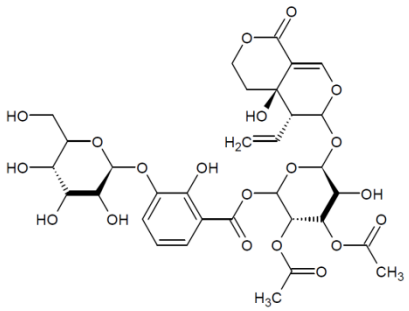	$C_{16}H_{22}O_8$	Coniferin
20	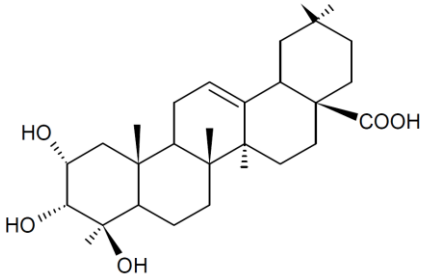	$C_{30}H_{48}O_5$	2α,3α,24-tri-hydroxyolean-12-en-28-oic acid
21	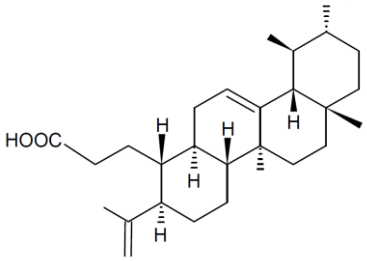	$C_{30}H_{48}O_2$	Roburic acid
22	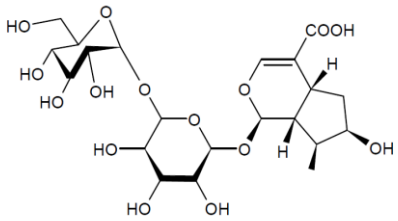	$C_{21}H_{32}O_{15}$	6′–O-β-D-glucosylloganic acid
23	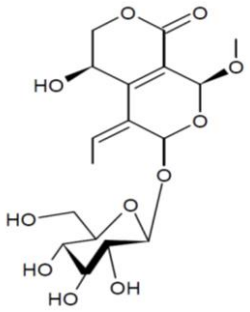	$C_{17}H_{24}O_{11}$	Qingjiaosides A
24	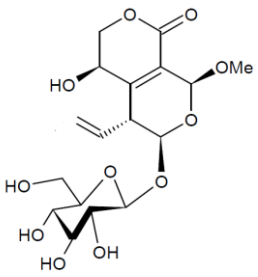	$C_{17}H_{24}O_{11}$	Qingjiaosides B

25	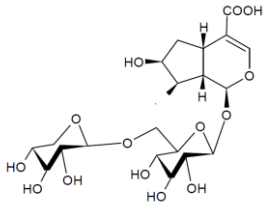	$C_{21}H_{32}O_{14}$	Qingjiaosides C
26	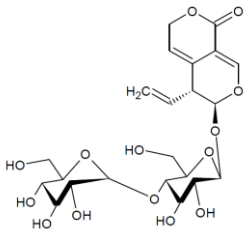	$C_{22}H_{30}O_{14}$	4′–O-β-D-glucosylgentiopicroside
27	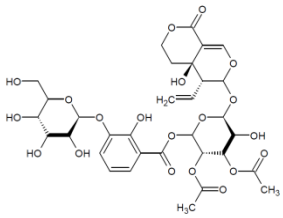	$C_{31}H_{36}O_{21}$	Macrophyllosides A
28	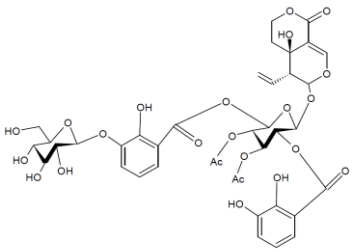	$C_{39}H_{42}O_{23}$	Macrophyllosides E
29	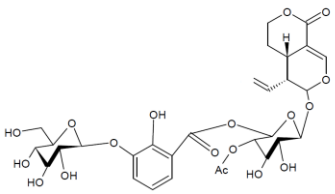	$C_{30}H_{36}O_{18}$	Macrophyllosides F
30	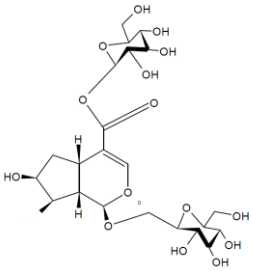	$C_{23}H_{36}O_{15}$	Loganic acid 11-O-β-D-glucopyranosyl ester
31	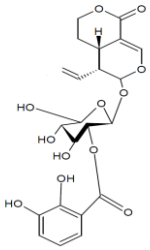	$C_{22}H_{24}O_{12}$	2-(o,mdi-hydroxybenzoyl)-sweroside

32	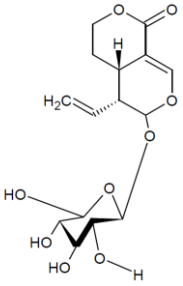	$C_{16}H_{22}O_9$	Sweroside
33	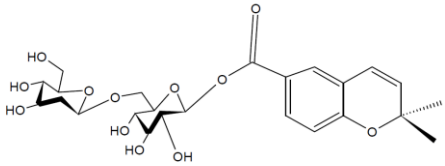	$C_{24}H_{32}O_{12}$	Macrophylloside D

Table 2: Biological activity predicted by PASS server for the thirty-three ligands.

S.no	Molecular formula	Name	Biological activity
1	$C_{38}H_{54}O_{21}$		Anti-inflammatory Nonsteroidal anti-inflammatory agent
2	$C_{16}H_{20}O_9$	Gentiopicroside	Anti-inflammatory Nonsteroidal anti-inflammatory agent
3	$C_{22}H_{30}O_{14}$	6′-O-β-D-glucopyranosyl gentiopicroside	Anti-inflammatory Nonsteroidal anti-inflammatory agent
4	$C_{27}H_{38}O_{19}$	Scarban G3	Anti-inflammatory Nonsteroidal anti-inflammatory agent
5	$C_{22}H_{30}O_{14}$	Olivieroside C	Anti-inflammatory Nonsteroidal anti-inflammatory agent
6	$C_{16}H_{22}O_{10}$	Swertiamarin	Anti-inflammatory Nonsteroidal anti-inflammatory agent
7	$C_{16}H_{26}O_9$	1-O-β-D-glucopyranosyl-amplexi	Anti-inflammatory Nonsteroidal anti-inflammatory agent
8	$C_{17}H_{24}O_{11}$	Epi-kingiside	Anti-inflammatory Nonsteroidal anti-inflammatory agent
9	$C_{17}H_{24}O_{11}$	Kingiside	Anti-inflammatory Nonsteroidal anti-inflammatory agent
10	$C_{16}H_{24}O_{10}$	Loganic acid	Anti-inflammatory Nonsteroidal anti-inflammatory agent
11	$C_{17}H_{26}O_{10}$	Loganin	Anti-inflammatory Nonsteroidal anti-inflammatory agent
12	$C_{27}H_{44}O_6$	Ajugasterone C	Anti-inflammatory Nonsteroidal anti-inflammatory agent
13	$C_{27}H_{44}O_7$	20-hydroxyecdysone	Anti-inflammatory Nonsteroidal anti-inflammatory agent
14	$C_{28}H_{46}O_8$	20-hydroxyecdysone 3-acetate	Anti-inflammatory Nonsteroidal anti-inflammatory agent
15	$C_{28}H_{36}O_{13}$	Syringaresinol-β-D-glucopyranoside	Anti-inflammatory Nonsteroidal anti-inflammatory agent
16	$C_{34}H_{46}O_{18}$	Liriodendrin	Anti-inflammatory Nonsteroidal anti-inflammatory agent
17	$C_{31}H_{40}O_{16}$	Dehydrodiconiferyl alcohol 4,γ′-di-O-β-D-glucopyranoside	Anti-inflammatory Nonsteroidal anti-inflammatory agent
18	$C_{20}H_{24}O_6$	Lariciresinol-4′-O-β-D-glucopyranoside	Anti-inflammatory Nonsteroidal anti-inflammatory agent
19	$C_{16}H_{22}O_8$	Coniferin	Anti-inflammatory

			Nonsteroidal anti-inflammatory agent
20	$C_{30}H_{48}O_5$	2α,3α,24-tri-hydroxyolean-12-en-28-oic acid	Anti-inflammatory Nonsteroidal anti-inflammatory agent
21	$C_{30}H_{48}O_2$	Roburic acid	Anti-inflammatory Nonsteroidal anti-inflammatory agent
22	$C_{21}H_{32}O_{15}$	6′–O-β-D-glucosylloganic acid	Anti-inflammatory Nonsteroidal anti-inflammatory agent
23	$C_{17}H_{24}O_{11}$	Qingjiaosides A	Anti-inflammatory Nonsteroidal anti-inflammatory agent
24	$C_{17}H_{24}O_{11}$	Qingjiaosides B	Anti-inflammatory Nonsteroidal anti-inflammatory agent
25	$C_{21}H_{32}O_{14}$	Qingjiaosides C	Anti-inflammatory Nonsteroidal anti-inflammatory agent
26	$C_{22}H_{30}O_{14}$	4′–O-β-D-glucosylgentiopicroside	Anti-inflammatory Nonsteroidal anti-inflammatory agent
27	$C_{31}H_{36}O_{21}$	Macrophyllosides A	Anti-inflammatory Nonsteroidal anti-inflammatory agent
28	$C_{39}H_{42}O_{23}$	Macrophyllosides E	Anti-inflammatory Nonsteroidal anti-inflammatory agent
29	$C_{30}H_{36}O_{18}$	Macrophyllosides F	Anti-inflammatory Nonsteroidal anti-inflammatory agent
30	$C_{23}H_{36}O_{15}$	Loganic acid 11-O-β-D-glucopyranosyl ester	Anti-inflammatory Nonsteroidal anti-inflammatory agent
31	$C_{22}H_{24}O_{12}$	2-(o,mdi-hydroxybenzoyl)-sweroside	Anti-inflammatory Nonsteroidal anti-inflammatory agent
32	$C_{16}H_{22}O_9$	Sweroside	Anti-inflammatory Nonsteroidal anti-inflammatory agent
33	$C_{24}H_{32}O_{12}$	Macrophylloside D	Anti-inflammatory Nonsteroidal anti-inflammatory agent

Table 3: Glide module details for the protein (COX-2) – ligand(s) complex.

S.No	Compound	Docking score	Glide Energy	No of H-bond	Residue	Residue Atom	Ligand Atom	Bond length
1	$C_{27}H_{38}O_{19}$	-14.47	-68.43	9	Leu 224	O	H	1.93
					Ser 143	O	H	1.62
					Ser 143	O	H	1.56
					Gly 225	O	H	2.09
					Asn 375	O	H	1.71
					Arg 376	H	O	2.26
					Gln 374	O	H	2.03
					Tyr 373	O	H	1.96
					Gly 536	H	O	0.96
2	$C_{21}H_{32}O_{15}$	-12.24	-56.19	5	Arg 376	H	O	1.92
					Ser 143	O	H	1.93
					Gly 225	O	H	2.16
					Gln 374	O	H	2.19
					Asn 375	O	H	1.84
3	$C_{24}H_{32}O_{12}$	-11.36	-63.31	3	Asn 375	O	H	2.22
					Arg 376	H	O	2.13
					Asp 229	O	H	2.93
4	$C_{23}H_{36}O_{15}$	-10.9	-67.82	3	Asn 375	O	H	2.39
					Arg 376	H	O	2.27
					Ser 143	O	H	2.13
5	$C_{22}H_{30}O_{14}$	-10.44	-55.84	4	Asn 375	O	H	2.18
					Arg 376	H	O	2.36
					Val 538	H	O	2.4
					Tyr 373	H	O	2.02
6	$C_{22}H_{24}O_{12}$	-10.35	-62.76	4	Gln 374	H	O	2.3
					Gln 374	H	O	1.98

					Gln 374	O	H	1.88
					Gln 374	O	H	2.11
7	$C_{22}H_{30}O_{14}$	-9.42	-61.39	6	Gly 225	O	H	2.02
					Gly 225	O	H	2.24
					Asn 375	O	H	2.02
					Arg 376	H	O	2.31
					Asn 375	O	H	1.94
					Asn 375	O	H	2.14
8	$C_{17}H_{26}O_{11}$	-9.31	-51.21	7	Asn 375	H	O	2.16
					Asn 375	O	H	2.12
					Arg 376	H	O	2.27
					Arg 376	H	O	2.16
					Gln 374	O	H	2.2
					Gln 374	O	H	7.37
					Gln 374	O	H	1.97
9	$C_{30}H_{36}O_{18}$	-8.65	-77.34	3	Val 538	H	O	2.07
					Arg 333	H	O	4.26
					Glu 236	O	H	1.78
10	$C_{17}H_{24}O_{11}$	-8.36	-47.67	4	Asn 375	H	O	2.14
					Asn 375	H	O	2.75
					Asn 375	H	O	2.35
					Arg 376	H	O	2.05
11	$C_{27}H_{44}O_{7}$	-8.3	-52.88	1	Gly 225	O	H	2.05
12	$C_{16}H_{20}O_{9}$	-7.25	-47.2	4	Arg 376	H	O	2.11
					Gln 374	O	H	2.28
					Gln 374	O	H	2.27
					Arg 376	H	O	2.27
13	$C_{16}H_{24}O_{10}$	-6.8	-43.58	4	Gly 225	O	H	2.01
					Arg 376	H	O	2.49
					Gly 225	O	H	2.08
					Ser 143	O	H	1.93
14	$C_{17}H_{24}O_{11}$	-6.14	-50.88	5	Gln 374	O	H	2.02
					Arg 376	O	H	3.23
					Asn 375	O	H	1.88
					Leu 224	O	H	1.93
					Arg 376	H	O	2.48
15	$C_{27}H_{44}O_{6}$	-5.85	-54.32	3	Gly 225	O	H	2.06
					Gly 225	O	H	2.5
					Asn 375	O	H	1.91
16	$C_{17}H_{24}O_{11}$	-3.95	-47.44	3	Asn 375	O	H	1.7
					Asn 375	O	H	2.29
					Asn 375	O	H	2.14
17	$C_{28}H_{46}O_{8}$	-3.84	-46.82	2	Asn 375	H	O	2.29
					Asn 375	O	H	1.97

RA whereas the flowers of *G. dahurica* are also known for the treatment of a sore throat, cough and lung disorders[18-19]. Wang et al (2013) reported the presence of iridoid glycosides, steroids, lignans, phenylpropanoid and triterpenes in *G. dahurica*. They also reported that the compounds present in *Gentiana* have potential inhibitory effects on 12-O-tetradecanoylphorbol-13-acetate (TPA) - induced COX-2 and COX-1 and lipopolysaccharides (LPS)-induced NO production through enzyme inhibitors screening assays[20]. Till now, there is no computational approach reported on these compounds against RA. Twenty-one compounds from *G. dahurica* (*Gentianaceae*) and twelve compounds from other *Gentiana species* were considered for *in silico* studies. The selected ligands were sketched using ISIS draw and 3D optimization was done through ChemSketch. Ligands preparation and docking was carried out using LigPrep and Glide modules of Maestro v 9.2. Predictive interaction models of these compounds with COX-2 protein were generated. Binding score, glide energy, hydrogen bonds and bond lengths were evaluated in order to find the lead compound. The best compound with the protein complex was subjected to molecular dynamic simulations using Desmond v4.0 for understanding its stability and confirmation.

MATERIALS AND METHODS

Target protein preparation

X-RAY crystallographic structure of mefenamic acid bound to human cyclooxygenase-2 (2.34 Å) was retrieved from Protein Data Bank (PDB ID: 5IKR) as the target

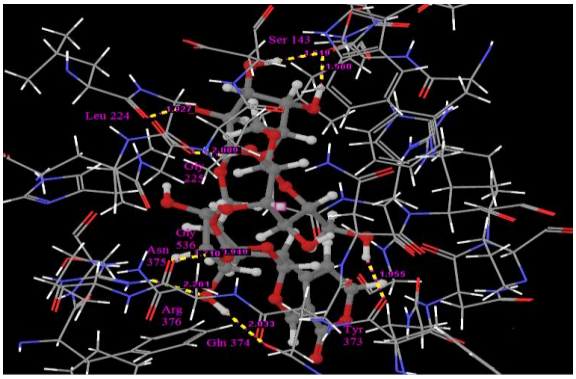

Figure 1: Interaction of $C_{27}H_{38}O_{19}$ with the active sites of the COX-2

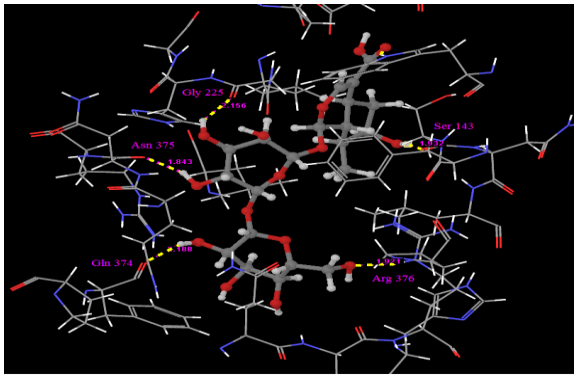

Figure 2: Interaction of $C_{21}H_{32}O_{15}$ with the active sites of the COX-2

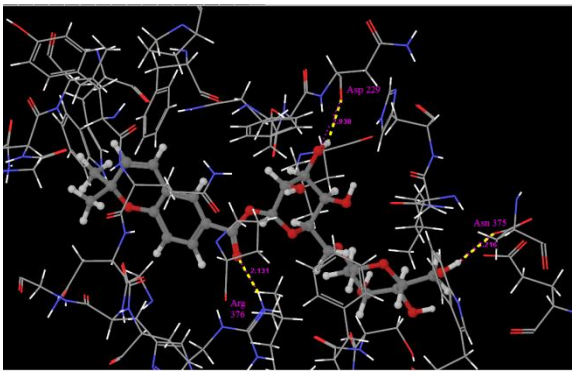

Figure 3: Interaction of $C_{24}H_{32}O_{12}$ with the active sites of the COX-2

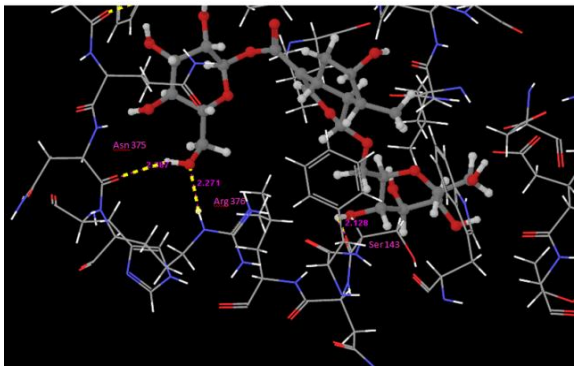

Figure 4: Interaction of $C_{23}H_{36}O_{15}$ with the active sites of the COX-2

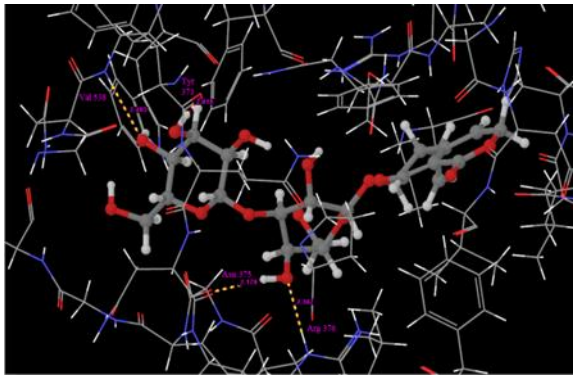

Figure 5: Interaction of $C_{22}H_{30}O_{14}$ with the active sites of the COX-2

protein for RA against inflammation. It contains A and B chains both with the length of 551 amino acids[21]. The active site amino acid information of the target protein was collected from PDBsum. Target protein was pre-processed using protein preparation wizard in Maestro v 9.2 interface. In the pre-processing step, all the ligands attached to the protein were removed along with water molecules. Prime tool was used to build the missing side chains in the protein structure. Optimized Potentials for Liquid Simulations (OPLS) force field and Polack-Ribiere Conjugate Gradient (PRCG) algorithm were used to obtain the optimized and minimized structure of the protein with the root mean square deviation (RMSD) value of 0.2 Å.

Preparation of compound libraries for Gentiana species

The thirty-three compounds reported by Wang et al (2013), were selected for the docking studies against COX-2. Among these, lignan glycoside, gentiopicroside, 6′-O-β-D-glucopyranosyl gentiopicroside, scarban G3, olivieroside C, swertiamarin, 1-O-β-D-glucopyranosyl-amplexi, epi-kingiside, kingiside, loganic acid, loganin, ajugasterone C, 20-hydroxyecdysone, 20-hydroxyecdysone 3-acetate, syringaresinol-β-D-glucopyranoside, liriodendrin, dehydrodiconiferyl alcohol 4,γ′-di-O-β-D-glucopyranoside, ariciresinol-4′-O-β-D-glucopyranoside, coniferin, 2α,3α,24-tri-hydroxyolean-12-en-28-oic acid and roburic acid were selected from *Gentiana dahurica Fisch* (Gentianaceae). Compounds 6′–O-β-D-glucosylloganic acid, qingjiaosides A–C and 4′–O-β-D-glucosylgentiopicroside were taken from *Gentiana crassicaulis.* macrophyllosides A, E–F, loganic acid 11-O-β-D-glucopyranosyl ester, macrophylloside D were obtained from *Gentiana straminea.* 2-(o,mdi-

Table 4: Pharmacological properties prediction of the docked ligands.

Compound	MW	Donor HB	Accpt HB	QPlog BB	QPlog Po/w	QPlogS	QPP MDC	QPP Caco	SASA	QPlog Kp
$C_{16}H_{20}O_9$	356.33	4	14.9	-1.80	-1.59	-1.42	34.51	85.13	558.07	-4.55
$C_{22}H_{30}O_{14}$	518.47	7	23.4	-3.53	-3.46	-1.34	2.94	8.71	749.83	-5.91
$C_{27}H_{38}O_{19}$	666.59	10	31.9	-3.94	-5.57	-0.19	2.19	6.44	805.63	-5.60
$C_{22}H_{30}O_{14}$	518.47	7	23.4	-3.37	-3.43	-1.24	3.76	10.94	738.02	-5.70
$C_{17}H_{24}O_{11}$	404.37	4	16.9	-2.38	-2.23	-1.64	12.45	33.15	617.86	-5.52
$C_{17}H_{24}O_{11}$	404.37	4	16.9	-2.31	-1.99	-1.82	16.45	42.89	635.41	-5.23
$C_{16}H_{24}O_{10}$	376.36	6	15.6	-2.53	-1.60	-1.87	2.34	5.64	594.98	-5.69
$C_{17}H_{26}O_{10}$	390.39	5	15.6	-2.01	-1.43	-2.07	43.98	106.55	631.57	-4.36
$C_{27}H_{44}O_6$	464.64	5	8.6	-1.70	-2.50	-4.13	85.66	197.43	702.45	-3.83
$C_{27}H_{44}O_7$	480.64	6	9.35	-2.01	-1.80	-3.41	35.48	87.34	682.48	-4.43
$C_{28}H_{46}O_8$	510.67	5	11.05	-2.01	-2.59	-4.90	95.49	218.30	812.19	-3.54
$C_{21}H_{32}O_{15}$	524.47	7	22.7	-3.48	-3.13	-1.94	0.53	1.434	729.13	-6.72
$C_{17}H_{24}O_{11}$	404.37	5	18.3	-1.61	-2.45	-0.71	42.46	103.14	517.13	-4.38
$C_{30}H_{36}O_{18}$	684.60	6	24.5	-4.57	-1.95	-3.00	1.74	5.37	974.81	-5.74
$C_{23}H_{36}O_{15}$	552.53	9	24.1	-4.49	-3.76	-1.82	0.98	3.17	830.94	-6.63
$C_{22}H_{24}O_{12}$	480.42s	3	17.25	-1.96	-1.31	-2.03	25.31	63.92	659.81	-4.51
$C_{24}H_{32}O_{12}$	512.51	6	18.05	-2.46	-0.85	-2.51	27.44	68.88	750.04	-4.04

hydroxybenzoyl)-sweroside and sweroside from *Gentiana rigescens*

Two-dimensional representations of all these thirty-three compounds were drawn using ISIS Draw 2.3 software (Table 1). Mol files of these thirty-three derivatives were created and their 3D optimization was done with the help of ChemSketch 3D viewer of ACD/Labs 8.0. Truncated Newton method was used to minimize the ligands in Maestro v 9.2 with "Molecular Mechanics Force Fields (OPLS)" algorithm. Potential energy, Max-Gradient, and RMS gradient cycles were analyzed during ligand minimization. Each ligand was optimized with different ring conformation, tautomerizer, ionization states, stereoisomers and their 3D structures were also generated by LigPrep (Schrödinger). These selected thirty-three ligands were also subjected to the prediction of their biological activity using PASS (Prediction of Activity Spectra for Substances) server which predicts the pharmacological effects of an individual compound [22].

Grid generation

Receptor grid generation was done using Glide by considering the active sites of the COX-2 target protein to allow the flexible movement of all the small molecules. The active site of the COX-2 protein was obtained using PDBsum. Interaction amino acids were taken for Grid generation which included Val46(A), His90(A), Tyr130(A), Ala199(A), Phe200(A), Phe201(A), Ala202(A), Gln203(A), His207(A), His214(A), Arg216(A), Lys243(A), Ala271(A), Glu272(A), Asp347(A), Val349(A), His351(A), Leu352(A), Ser353(A), Asn382(A), Tyr385(A), His386(A), Trp387(A), His388(A), Leu391(A), Ala405(A), Val447(A), Arg513(A), Ala516(A), Ile517(A), Phe518(A), Met522(A), Val523(A), Gly526(A), Ala527(A)

Docking procedure

All the 33 ligands were virtually screened against COX-2 protein using Schrodinger Glide module. Each ligand was evaluated by Glide standard precision mode (Glide SP) with respect to their best 5 poses and their corresponding scores. Ligands with the least Glide SP score were selected and given as inputs for the Glide docking in extra precision mode (Glide XP). Van der Waals radius was set with the scale of 1.0 with a partial cut-off of 0.25 in spite of providing the non polar parts of the receptor with the soften potential. Shape comparison filter, along with Monte Carlo conformational search helped to generate different ligand confirmations with the active site shape. Lowest glide score for various poses of each ligand was re-scored with the help of MM-GBSA (Molecular mechanics-generalized Born and surface area continuum salvation) rescoring approach. Binding free energy (ΔG_{bind}) was calculated by finding the deviation between the energy of the complex and total energies of the ligand and unliganded receptor[23].

$$\Delta G_{bind} = E_{R:L} - (E_R + E_L) + \Delta G_{solv} + \Delta G_{SA}$$

where $E_{R:L}$ represents the total energy of the both receptor and ligand, $E_R + E_L$ denotes the sum of ligand and receptor energies, ΔG_{solv} (ΔG_{SA}) represents the deviation between the GBSA solvation energy of the docking complex and sum of the corresponding energies for the ligand and target protein.

ADME & Lipinski rule

Significant pharmacological properties like absorption, distribution, metabolism, and excretion (ADME) decide the bioactivity for candidate drugs. All the ligands were evaluated for favorable ADME properties and Lipinski's rule [24] by using Schrodinger QikProp module[25]. Integration of ADME predictions in the drug development process leads to the generation of potential drug which may elicit required ADME performances. Donor hydrogen bond, acceptor hydrogen bond, molecular weight, total SASA, partition coefficient between octanol and water (QP logPo/w), solubility (QPlogS), QP logKp for skin permeability, Caco-2-permeability (QPP Caco), QP logBB (brain blood partition coefficient) for Brain/Blood and QPP MDCK (Madin-Darby Canine Kidney Epithelial

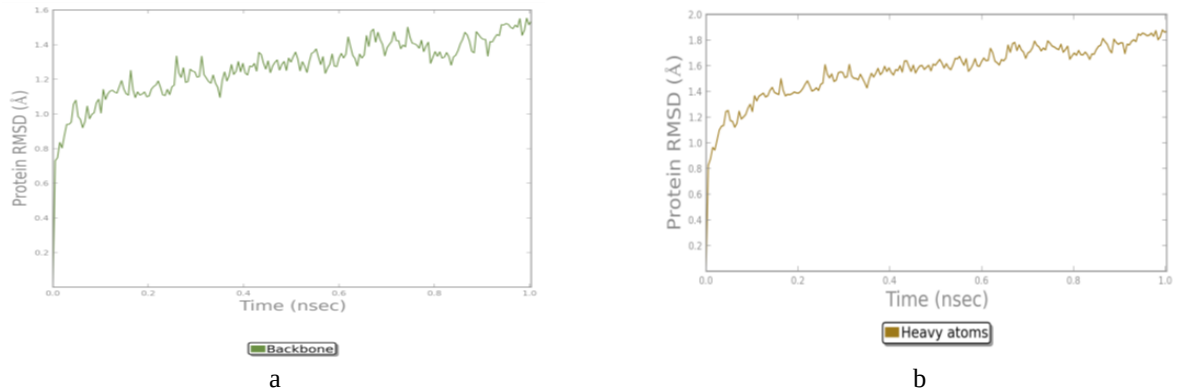

a b

Figure 6: (a): RMSD of backbone atoms of the COX-2 protein with $C_{27}H_{38}O_{19}$ during the MD simulation **(b)** RMSD of heavy atoms of the COX-2 protein with $C_{27}H_{38}O_{19}$.

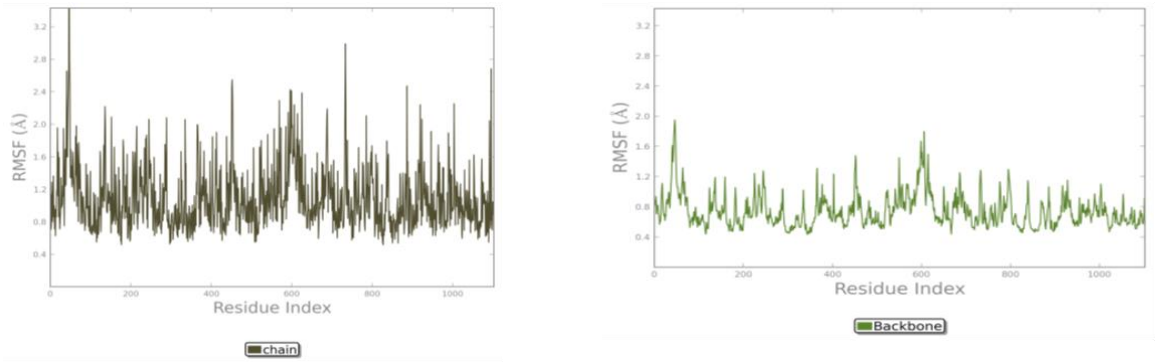

a b

Figure 7: (a): RMSF of backbone atoms of the COX-2 with $C_{27}H_{38}O_{19}$ MD simulation **(b)** RMSF of side chain atoms of the COX-2 with $C_{27}H_{38}O_{19}$ MD simulation.

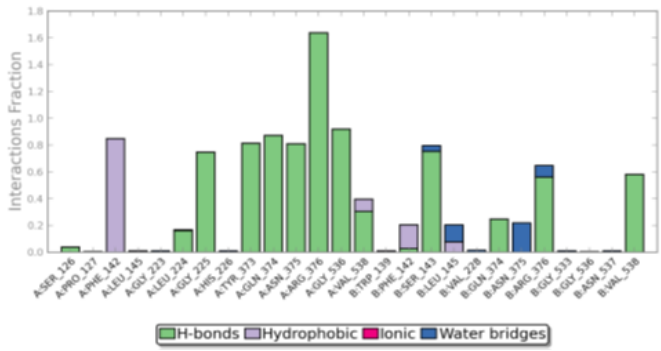

Figure 8: plot of COX-2 AND ligand $C_{27}H_{38}O_{19}$ contracts MD simulation.

Cells) were evaluated for all the docked ligands. For a candidate drug, molecular weight should be less than 500 Da, QPlogS should be less than four, hydrogen bond donor is less than 5, and hydrogen bond acceptor should be less than 10. QPlogBB indicates the capability of a drug to penetrate the blood barrier. QPP MDCK calculates the MDCK cell permeability in nm/s. High value of MDCK cell represents the high cell permeability[26].

Molecular dynamics (MD) simulation

The stability and conformational changes of compound $C_{27}H_{38}O_{19}$ with respect to the active site of COX-2 were determined by MD simulations using Desmond v 4.0 software[27]. OPLS force field was used to represent the amino acid interaction in COX-2. SPC (simple point charge) method was applied in the water model[28]. Orthorhombic box with the volume of 100 Å *100 Å *100 Å was built using system builder in Desmond and SPC water molecules were added into it. Na^+ and Cl^- counter ions were also added to the system in order to neutralize it. After solvent environment is constructed, the entire system consisted of 102466 atoms. Parameters such as Number of atoms, Pressure and Temperature (NPT) was taken into account in the minimization of the entire complex. Particle mesh Ewald method was used to evaluate the interactions between the molecules in the long range[29]. The whole complex was subjected to 1 ns simulation at 300K. Structural changes and dynamic behavior of the complex were evaluated using different parameters including RMSD and root mean square fluctuations (RMSF).

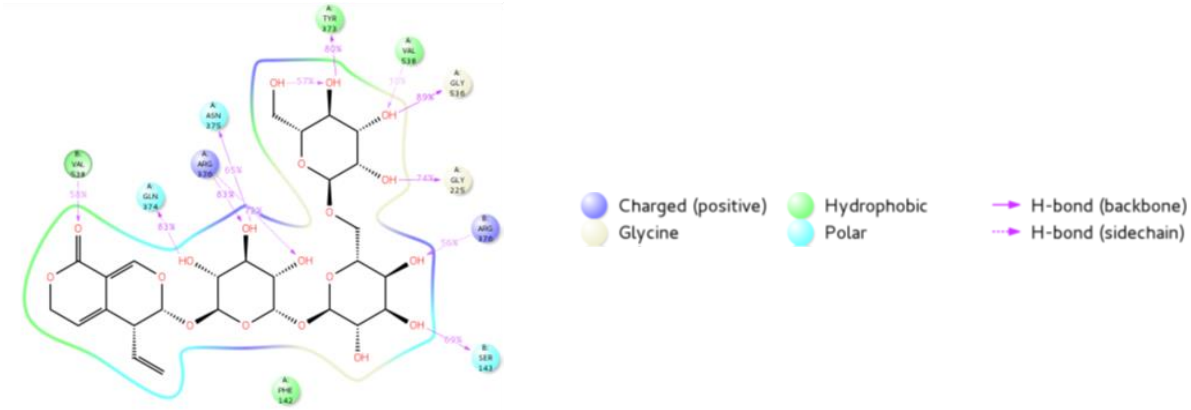

Figure 9: Overall Interaction between residues of COX-2 protein with $C_{27}H_{38}O_{19}$ complex during MD simulation.

RESULTS AND DISCUSSION

Glide docking

Three-dimensional crystal structure of COX-2 protein was downloaded from PDB and the active sites were retrieved from PDBsum Database. The protein is attached to five ligands and one ion: Mefenamic acid, Protoporphyrin IX containing co, N-Acetyl-D-Glucosamine, B-Octylglucoside and Ammonium ion. Interacting amino acids between the ligand and protein were obtained from LIGPLOT. Interaction sites of all these five ligands were taken as active site box for the docking of thirty-three derivatives of Gentiana species in the present study. The biological activity of the thirty-three selected ligands obtained using pass server indicated that all the compounds are having the anti-inflammatory activity and also they can act as nonsteroidal anti-inflammatory agents as shown in Table 2.

The target protein and thirty-three ligands were docked in both Standard-precision (SP) and extra-precision (XP) docking modes. During the first mode, several conformations of ligands with restricted variation around acyclic torsion bonds, pyramidal nitrogen inversions, and ring conformations were generated internally during SP-flexible docking process. Only low energy conformations were participated in the docking. Among thirty-three ligands, seventeen ligands were docked with the target protein. Ligand poses of compounds with minimum glide energy were used as inputs for XP docking with Refine (do not dock) mode. Ligand coordinates of the input were optimized in the orbit of the receptor. The least XP docking score was selected as the best lead. Compound $C_{27}H_{38}O_{19}$ has the least docking score = -14.47 and the glide energy is -68.43KcaL/mol. Nine hydrogen bonds were formed with the COX-2 target protein at the residues Leu 224, Ser 143, Ser 143, Gly 225, Asn 375, Arg 376, Gln 374, Tyr 373 and Gly 536 with the bond length of 1.93 Å, 1.62 Å, 1.56 Å, 2.09 Å, 1.71 Å, 2.26 Å, 2.03 Å, 1.96 Å, 0.96 Å respectively (Figure. 1). Zarghi et al (2011) reported that the active sites of COX-2 protein were found in the range from Arg 120 to Tyr 385 which is present in the upper half of the channel. Current docking results also exhibited the same binding sites. Compound $C_{27}H_{38}O_{19}$, compound $C_{21}H_{32}O_{15}$, compound $C_{24}H_{32}O_{1,}$ compound $C_{23}H_{36}O_{15}$ and compound $C_{22}H_{30}O_{14}$ are top five lead compounds which have minimum docking score (Figure. 2, 3, 4, 5). Details of the hydrogen bond, bond length, docking score and glide energy for all the ligands are shown in Table 3.

Pharmacology prediction

Lipinski rule of five along with total SASA, QPlog MDCK, QP logS, QP logKp and QPP Caco-2 was used to calculate pharmacodynamics properties which evaluate bioactivity of the potential lead compounds. All the ligand molecules showed the molecular weight in the average of 534.52 Dalton. Predicted aqueous solubility, blood-brain barrier, QPlog MDCK, skin permeability, total SASA, and gut-blood barriers were found to be in the acceptance range. From the interpretation of the results obtained by docking and pharmacology prediction studies, Compound $C_{27}H_{38}O_{19}$ can be used as the potential candidate drug in relation to the inflammatory process occurring during RA as shown in Table 4.

Molecular dynamics simulations of COX-2 and $C_{27}H_{38}O_{19}$

Molecular dynamics simulations were carried out for the compound $C_{27}H_{38}O_{19}$ with COX-2 complex to evaluate conformational stability, molecular compactness, and dynamic properties in the real time environment. The solvent environment of water molecules, Na^+ and Cl^- ions, appropriate temperature, and pressure were applied to the docking complex by the simulation algorithm. The simulation was carried out with the appropriate binding poses along with an acceptable RMSD range of less than 3 Å. RMSD graph elucidated the stability of the protein during the ligand interaction. RMSD value for heavy atoms ranges from 0.82–1.86 Å (Figure. 6(a)) and for back-bone atoms 0.73–1.55 Å (Figure. 6(b)) throughout the simulation. RMSF value for every residue in the COX-2 protein was evaluated based on the average of all the atoms of the given residue. RMSF was calculated for side chain and backbone residues (Figure. 7(a, b)). The RSMF value for backbone residues was in the range of 0.44–1.87 Å and side chain residues were in 0.52–2.33 Å. The total energy of the system, potential energy, temperature, pressure and volume were found during the simulation studies as 2196.732 kcal/mol, 7574.479 kcal/mol, 298.640 K, 0.008 bar and 5748.201 $Å^3$, respectively.

Analysis of bonded interaction of $C_{27}H_{38}O_{19}$ with COX-2 complex

The four different possible interactions between COX-2 and $C_{27}H_{38}O_{19}$ were examined during the MD simulations (Figure 8). These interactions were H-bond, hydrophobic, ionic interactions and water bridges. H-bond plays a crucial role in drug development and has a strong influence on drug specificity, metabolism, and absorption. More hydrogen bonds indicate more stable interaction. Hydrogen bond interactions were found at Leu 224, Gly 225, Tyr 373, Gln 374, Asn 375, Gly 536, Val 538, Phe 142, Seq 143, Gln 374 and Agr 376. Hydrophobic interactions were found at the residue of Phe 142, Val 538 and Leu 145, whereas water bridges were found at Ser 143, Leu 145, Val 228, Asn 375 and Arg 376. No ionic interactions were found during the interactions. Among all the possible interactions, totally nine hydrogen bonds were formed between $C_{27}H_{38}O_{19}$ and COX-2 (Figure 9) during simulation studies. $C_{27}H_{38}O_{19}$ forms hydrogen bonds with Val 538, Ser 143, Gly 225, Asn 375, Arg 376, Gln 374, Tyr 373, Arg 376 and Gly 536 of COX-2. The H-bond interactions were in equilibrium state throughout the simulation period. From the understanding of docking and MD simulation, $C_{27}H_{38}O_{19}$ ligand has represented as the best conformational molecule in sense of stability and binding energy.

CONCLUSION

The main aim of this present work was to analyze the inhibitory effect of thirty-three compounds from Qin-Jiao and related *Gentiana* species against COX-2 through molecular modeling and simulation approaches. The target protein and ligands were minimized and the optimized ligands were further docked against COX-2 target protein. The results of docking study showed the best binding affinity between the compound $C_{27}H_{38}O_{19}$ with COX-2 target protein having minimum docking score and glide energy. The lead docked complex was further subjected to MD simulation using Desmond v 4.0 to evaluate the conformational stability. Throughout the MD simulations, hydrogen bond interactions were found between Val 538, Ser 143, Gly 225, Asn 375, Arg 376, Gln 374, Tyr 373, Arg 376 and Gly 536 of $C_{27}H_{38}O_{19}$ with COX-2. The study of potential energy, RMSF, and RMSD value for docking complex also established the stability of docked complex. Hence, this elicited the stability of the complex of COX-2 and $C_{27}H_{38}O_{19}$ in physiological environmental conditions. Pharmacological properties of the compound $C_{27}H_{38}O_{19}$ also showed the drug-like properties for being a potent drug. In future, this study can be taken over to *in vivo* and *in vitro* approaches for the treatment of RA in relation to inflammatory progression.

ACKNOWLEDGMENTS

This research work was supported and funded by Science and Engineering Research Board—Department of Science and Technology (SERB-DST) and Karunya University

CONFLICT OF INTEREST

We confirm that this manuscript has not been published elsewhere and there is no conflict of interest for this research

REFERENCES

1. Kahlenberg JM, Fox DA. Advances in the medical treatment of rheumatoid arthritis. Hand Clinics 2011; 27(1):11-20. doi: 10.1016/j.hcl.2010.09.002
2. Newsome G. American College of Rheumatology. Guidelines for the Management of Rheumatoid Arthritis. Journal of the American Association of Nurse Practitioners 2002; 14(10):432-7
3. Firestein GS. Evolving concepts of rheumatoid arthritis. Nature 2003; 423(6937):356-61
4. Choy EH, Panayi GS. Cytokine pathways and joint inflammation in rheumatoid arthritis. The New England Journal of Medicine 2001; 344(12):907-916
5. Bellucci E, Terenzi R, La Paglia GM, Gentileschi S, Tripoli A, Tani C, Alunno A. One year in review 2016: pathogenesis of rheumatoid arthritis. Clinical and Experimental Rheumatology 2016; 34(5):793-801
6. Rathore B, Ali Mahdi A, Nath Paul B, Narayan Saxena P, Kumar Das S. Indian herbal medicines: possible potent therapeutic agents for rheumatoid arthritis. Journal of Clinical Biochemistry and Nutrition 2007;41(1):12-17. doi: 10.3164/jcbn.2007002
7. Fu JY, Masferrer JL, Seibert K, Raz A, Needleman P. The induction and suppression of prostaglandin H2 synthase (cyclooxygenase) in human monocytes. The Journal of Biological Chemistry 1990; 265(28):16737-740
8. Konturek PC, Kania J, Burnat G, Hahn EG, Konturek SJ. Prostaglandins as mediators of COX-2 derived carcinogenesis in gastrointestinal tract. Journal of Physiology and Pharmacology 2005; Suppl 5:57-73
9. Martel-Pelletier J, Pelletier JP, Fahmi H. Cyclooxygenase-2 and prostaglandins in articular tissues. Seminars in Arthritis and Rheumatism 2003; 33(3):155-167
10. Crofford LJ. COX-1 and COX-2 tissue expression: implications and predictions. Journal of Rheumatology 1997; Suppl 49:15-19
11. Picot D, Loll PJ, Garavito RM. The X-ray crystal structure of the membrane protein prostaglandin H2 synthase-1. Nature 1994 367:243-249
12. Negrei C, Bojinca V, Balanescu A, Bojinca M, Baconi D, Spandidos DA, Tsatsakis AM, Stan M. Management of rheumatoid arthritis: Impact and risks of various therapeutic approaches. Experimental and Therapeutic Medicine 2016; 11(4):1177-1183
13. Moreland L, Baumgartner S, Schiff M, Tindall E, Fleischmann R, Weaver A, Ettlinger R, Cohen S, Koopman W, Mohler K, Widmer M, Blosch C. Treatment of rheumatoid arthritis with a recombinant human tumor necrosis factor receptor (p75)-Fc fusion protein. New England Journal of Medicine 1997; 337:141-147
14. Soeken KL, Miller SA, Ernst E. Herbal medicines for the treatment of rheumatoid arthritis: a systematic review. Rheumatology(Oxford) 2003; 42:652-659
15. Pharmacopoeia Committee of P.R. China. Pharmacopoeia of People's Republic of China. Chemical Industry Publishers, Beijing 2010; 253-254

16. Cai QS, Zhang ZH, Gao HQJ. 10) Gansu Coll. Journal of Traditional Chinese Medicine 2010; 27:55-58
17. Liu FF, Wang YM, Zhu HT, Wang D, Yang CR, Xu M, Zhang YJ. Comparative Study on Long-Dan, Qin-Jiao and Their Adulterants by HPLC Analysis. Natural Products and Bioprospecting 2014; 4(5):297-308. doi: 10.1007/s13659-014-0039-x
18. Li T, Zhang ZQ, Wang JZ. Utilization and protection of Chinese medicine Radix Gentianae macrophyllae. Shaanxi Journal of Agricultural Sciences 2006; 6:36-38
19. Fan H, Zang Y, Zhang Y, Zhang HF, Zhao Z, Hu JF (2010) Triterpenoids and iridoid glycosides from Gentiana dahurica. Helvetica Chimica Acta 2010; 93, 2439-2447
20. Wang YM, Xu M, Wang D, Yang CR, Zeng Y, Zhang YJ. Anti-inflammatory compounds of Qin-Jiao, the roots of Gentiana dahurica (Gentianaceae). Journal of Ethnopharmacology 2013; 147(2):341-348 doi: 10.1016/j.jep.2013.03.016
21. Orlando BJ, Malkowski MG. Substrate-selective Inhibition of Cyclooxygeanse-2 by Fenamic Acid Derivatives Is Dependent on Peroxide Tone. Journal of Biological Chemistry 2016; 291:15069-15081
22. Poroikov VV, Filimonov DA, Ihlenfeldt WD, Gloriozova TA, Lagunin AA, Borodina YV, Stepanchikova AV, Nicklaus MC. PASS biological activity spectrum predictions in the enhanced open NCI database browser. Journal of Chemical Information and Modeling 2002; 43(1):228-236
23. Genheden S, Ryde U. The MM/PBSA and MM/GBSA methods to estimate ligand-binding affinities. Expert Opinion on Drug Discovery 2015;10(5): 449-461
24. Lipinski CA, Lombardo F, Dominy BW, Feeney PJ. Experimental and computational approaches to estimate solubility and permeability in drug discovery and development settings. Advanced Drug Delivery Reviews 1997; Rev 23:3-25
25. QikProp3.2, Schrodinger LLC 2009; New York NY
26. Husain A, Khokra SL, Thakur P, Choudhary D, Kohli S, Ahmad A, Khan SA. Molecular Modeling and In Silico Evaluation of Novel Pyridazinones Derivatives as Anticonvulsant Agents. Journal of In Silico & In Vitro Pharmacology 2015; 1:1-7
27. Shan Y, Kim ET, Eastwood MP, Dror RO, Seeliger MA, Shaw DE. How does a drug molecule find its target binding site?. Journal of the American Chemical Society 2011; 133(24):9181-3.
28. Kaminski GA, Friesner RA, Tirado-Rives J, Jorgensen WL. Evaluation and reparametrization of the OPLS-AA force field for proteins via comparison with accurate quantum chemical calculations on peptides. Journal of Physical Chemistry B 2001; 105(28):6474-6487
29. Strahan GD, Keniry MA, Shafer RH. NMR structure refinement and dynamics of the K+-[d(G3T4G3)]2 quadruplex via particle mesh Ewald molecular dynamics simulations. Biophysical Journal 1998; 75(2):968-81
30. Zarghi A, Arfaei S. Selective COX-2 Inhibitors: A Review of Their Structure-Activity Relationships. Iranian Journal of Pharmaceutical Research 2011; 10(4): 655-683